struction, based on the exterior surface ribbing, yields a reduction in the variation of T_{eff} and provides for a control of the mean value of T_{eff}. It is possible to apply inclined ribs and ribs of different heights to provide a redistribution of the absorbed solar radiation on the exposed exterior surface.

The advantages of the considered modification decline for β near 0 and 180 deg. However, when the spacecraft operates on the orbit, the effect of external conditions is diminished due to the thermal inertia of the telescope. Therefore, more strict requirements should not be specified to obtain uniformity of the effective temperature.

References

[1]Mason, P. V., "Long-Term Performance of the Passive Thermal Control Systems of the IRAS Spacecraft," *Cryogenics*, Vol. 28, No. 2, 1988, pp. 137–141.

[2]Youdale, J., "State of the Art of ISO," *Cryogenics*, Vol. 29, No. 5, 1989, pp. 528–534.

[3]Murakami, M., Okuda, H., Matsumoto, T., Fujii, G., and Kyoya, M., "Design of Cryogenic System for IRTS," *Cryogenics*, Vol. 29, No. 5, 1989, pp. 553–558.

[4]Akau, R. L., and Larson, D. W., "Thermal Control of Space X-Ray Experiment," *Journal of Spacecraft and Rockets*, Vol. 26, No. 5, 1989, pp. 297–302.

[5]Siegel, R., and Howell, J. R., "Thermal Radiation Heat Transfer," McGraw–Hill, New York, 1972.

Study of Transpiration Cooling over a Flat Plate at Hypersonic Mach Numbers

Sreekanth* and N. M. Reddy†
Indian Institute of Science, Bangalore 560 012, India

Nomenclature

C_h = Stanton number
E = relative change
h = enthalpy
k = thermal conductivity
M = Mach number
$\dot{m}$ = mass injection rate
$\dot{q}$ = heat flux
Re = Reynolds number
T = temperature
x = distance along the plate measured from the leading edge
y = distance normal to the surface (also y coordinate)

Subscripts
a = aerodynamic
C = coolant
r = recovery
W = wall
∞ = freestream

Superscripts
$*$ = dimensional quantities
est = estimated value

Received April 22, 1994; presented as Paper 94-2075 at the AIAA/ASME Joint Thermophysics and Heat Transfer Conference, Colorado Springs, CO, June 20–23, 1994; revision received Nov. 16, 1994; accepted for publication Dec. 12, 1994.

*Research Scholar, Department of Aerospace Engineering; currently Engineer of VSSC.

†Professor, Department of Aerospace Engineering. Associate Fellow AIAA.

Introduction

AERODYNAMIC heating is a major concern in the design of hypersonic transport vehicles. Although various cooling systems have been adopted in the past to protect the vehicle from excessive heating, their usage with respect to the concept of hypersonic transport is doubtful. Hence, alternative forms of cooling systems have to be evolved. A comparative study of various cooling systems made by McConarty and Anthony[1] indicated that the transpiration cooling system, on which the present study is focused, has the potential to cool the hypersonic cruise vehicles effectively. Although the literature on this subject is very rich, most of the theoretical work done was based on approximate equations such as boundary-layer and viscous shock-layer equations. Apart from this, many of these analyses were restricted to a particular region in the flowfield, such as the stagnation point. These analyses, in spite of the approximations involved at various levels, have given very good physical insight into the subject. Nevertheless, owing to the approximations made in these analyses, their results will have limited applications. Often it is difficult to say whether the solutions obtained through these analyses are unique or not,[2] unless a less approximate analysis confirms it. Moreover, for cases where flow separation occurs or a shock–shock or shock–boundary-layer interaction occurs, such an analysis cannot be made. In essence, there is an overall need for making a more accurate study of transpiration cooling. Recently, Sreekanth and Reddy[3] made a study based on Navier–Stokes equations. This Note is a short version of Ref. 3.

Problem Statement

The objective of the present work is to perform transpiration cooling analysis using Navier–Stokes equations. Also, unlike the earlier studies, the present work does not assume an isothermal wall with a prescribed wall temperature. Instead, the temperature of the coolant in the storage T_C^* is prescribed and the wall temperature T_W^* is obtained as a solution for this coolant temperature. In the authors' opinion this situation mimics the actual situation more realistically than the earlier studies.

The transpiration cooling mechanism can be classified into two phases. In the first phase (preinjection phase), the coolant temperature is raised from its storage value T_C^* to the value at the surface T_W^* by absorbing some of the oncoming heat. In the second phase (postinjection phase), the injected gas mixes with boundary-layer gas and partially blocks the heat transfer to the surface itself. In the present work, the wall temperature is calculated assuming that the coolant absorbs all the heat coming into the surface in the preinjection phase of cooling. Under such conditions, the heat balance at the surface leads to $\dot{q}_a^* = -\dot{q}_C^*$, where $\dot{q}_a^*$ is the aerodynamic heat load and $\dot{q}_C^*$ is the heat gained by the coolant before injection. By using appropriate expressions for $\dot{q}_a^*$ and $\dot{q}_C^*$ we get

$$k^* \frac{\partial T^*}{\partial y^*} = \dot{m}_W^*(h_W^* - h_C^*) \tag{1}$$

Eq. (1) is written in dimensional form. It should be noted that in the absence of gas injection, Eq. (1) leads to adiabatic wall condition. In this Note, the situation represented by Eq. (1) is referred to as the "no net heat flow into the wall" condition. Transpiration cooling analysis has been made for

flow over a flat plate placed along the flow direction. The study is limited to air transpiration with its initial temperature T_C^* equal to the ambient temperature T_∞^*. Mach numbers in the range of 6–10 and Reynolds numbers in the range of 10^6–10^7 have been chosen. The selection of the Mach number and the Reynolds number range was based on the trajectory of a typical re-entry vehicle and corresponds to an altitude of 30–50 km.[4] Although the high Reynolds numbers used warrant turbulence modeling, in the present work we have confined our research to laminar flows as a first step to study this complex interaction problem.

Numerical Algorithm and Validation

Two-dimensional full Navier-Stokes equations are cast in the integral form. The velocities are nondimensionalized with the freestream velocity, pressure with twice the freestream dynamic pressure, density, and temperature with the corresponding freestream quantities. The coordinates are nondimensionalized with a reference length L^*. Unlike a blunt body, which offers a definite length scale such as radius of the nose for reference length, flat plate does not offer any such length scale. It is sufficient to mention that x^* and y^* have been nondimensionalized with some reference length L^*. The important parameter for a flat plate is the local Reynolds number and this can be readily obtained by multiplying the freestream Reynolds number with x. The governing equations are discretized in the finite volume network. The inviscid terms are treated using Roe's flux difference scheme.[5] The accuracy of this scheme is enhanced using the MUSCL scheme[6] with $\kappa = \frac{1}{3}$. Viscous terms are treated using an auxiliary cell approach.[7] The temporal discretization is carried out in Euler-implicit form. Line–Jacobi relaxation algorithm has been applied to the resulting set of equations. The details of the boundary conditions used are available in Ref. 3. The Navier–Stokes code is validated against the available results for a variety of test cases. The details are available in Refs. 3 and 4. A nonsimilar boundary-layer code was also developed for the purpose of validating the Navier–Stokes code in the presence of transpiration.[4] Before proceeding for transpiration cooling studies, a grid refinement study was made to determine the accuracy of the Navier–Stokes code along the lines of Blottner.[8] The details of the grid refinement study are available in Ref. 4. It was found that in the finest grid chosen, the error in various quantities such as skin friction coefficient, wall pressure, and T_W were less than 5%, which is an acceptable one. Based on the grid refinement studies, 32 cells were used along the surface and 88 cells were used normal to the surface. The cell areas varied in both the directions. The details are given in Ref. 4.

Results and Discussion

Mass injection rate is a parameter in the analysis of transpiration cooling. Although it can be fixed arbitrarily, a new method has been suggested to select a useful range of blowing rates in the present work. Conceptually, this method aims at approximately determining the blowing rate required to achieve a desirable wall temperature at a given location along the plate. The details of this method are presented in Ref. 3. The final expression for the mass injection rate is

$$\dot{m}_W = C_{h0}[K/(B - K)] \tag{2}$$

where $K = (T_r - T_W)/(T_r - 1)$ and $B = (T_r - T_C)/(T_r - 1)$. This equation is valid for $B > K$. K by definition is the ratio of difference between the recovery temperature and the wall temperature expressed as a fraction of the difference between the recovery temperature and the freestream temperature. Equation (2) gives the approximate mass injection rate required to get a desired value of K at a location on the flat plate. In the present work blowing rate $\dot{m}_W$ is held constant along the flat plate and is calculated by the previous method for different values of K expected to prevail at $x = 1$ for $M_\infty = 6$ and $Re_\infty = 10^6$. For other Mach and Reynolds numbers, the same blowing rates as used for $M_\infty = 6$ and $Re_\infty = 10^6$ are used so as to facilitate parametric analysis. Although much experimental work has been done in the past, none of these results could be compared with them because most of the experimental results are available for axisymmetric body shapes and isothermal wall cases.

In Figs. 1a–1c, the quantity T_W is plotted at various blowing rates for different freestream conditions. As the blowing rate is increased, the wall temperature decreases at all locations. However, the magnitude of reduction in wall temperature decreases towards the leading edge. Similar trends are observed for other Mach numbers also and are reported in Ref. 3. Comparing Figs. 1a–1c, it can be said that blowing a cold gas becomes much more effective if Re_∞ is higher. Also, T_W has reached the storage temperature of coolant T_C in some portions of the flat plate for some blowing rates at $Re_\infty = 5 \times 10^6$ and 10^7. It appears from these figures that T_W depends on local Reynolds number Re_x at a given blowing rate and M_∞. Similar observations were also made for skin friction coefficient.[3]

In the study of transpiration cooling, change in a quantity due to blowing relative to the corresponding quantity with no blowing is important. The relative change in a quantity, e.g., Z, is defined as $E_Z = (Z - Z_0)/Z_0$, where Z is any quantity such as T_W with transpiration and Z_0 is the same quantity without transpiration. In Figs. 2a–2d, the relative change in T_W, i.e., E_T, due to blowing, are plotted for various freestream conditions and at different blowing rates. The relative change plots will help in comparing the effect of blowing at various freestream conditions. It can be observed that E_T is negative in all the graphs indicating that the gas injection reduces the wall temperature. Also, for a given blowing rate, E_T decreases along the surface and this decrease becomes more and more prominent at higher blowing rates, a fact that was evident from Figs. 1a–1c. At lower blowing rates, M_∞ has an insignificant effect on the E_T in all the regions of the plate. At higher blowing rates and only in regions away from the leading edge, E_T decreases with M_∞. Contrary to the effect of M_∞, Re_∞ has a significant effect on E_T in all the regions of the plate and at all the blowing rates. At higher Re_∞, E_T reduces to a limiting value at some blowing rates.

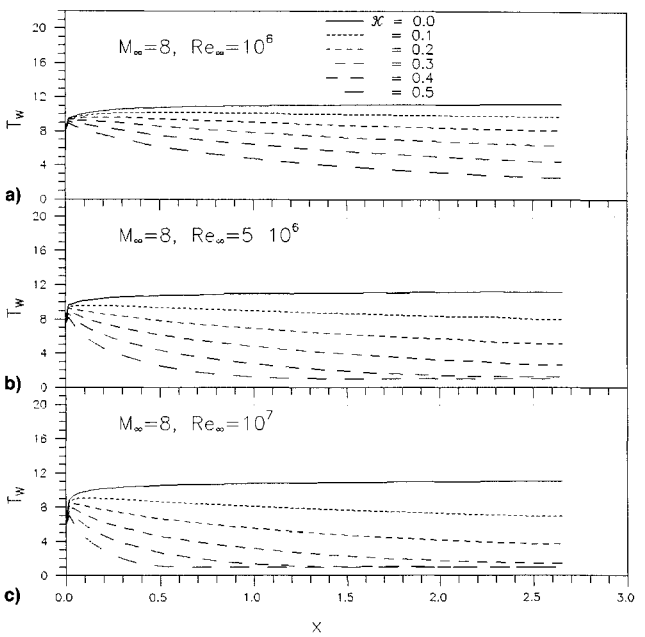

Fig. 1 T_W variation along the plate.

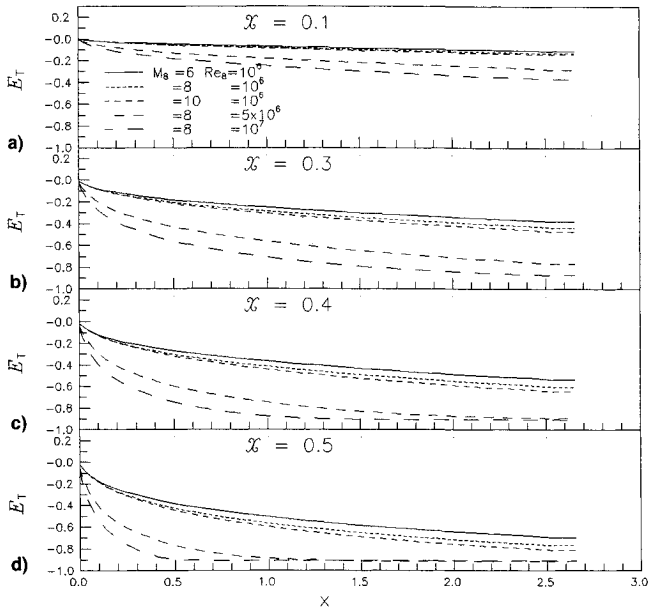

Fig. 2 E_T variation along the plate.

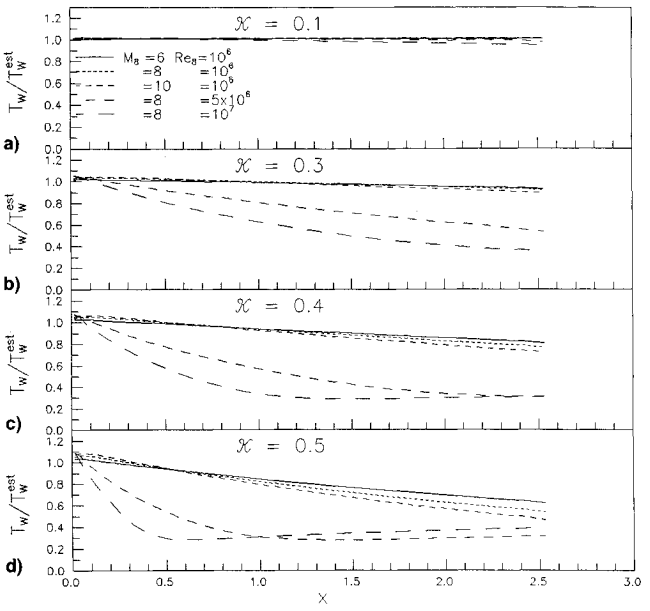

Fig. 3 T_W/T_W^{est} variation along the plate.

As explained earlier, the mechanism of cooling can be classified into two phases: 1) preinjection phase and 2) postinjection phase. Under the "no net heat flow into the wall" condition, the resulting wall temperature is due to the effect of both the phases, and unlike the case of isothermal wall, they are not clearly distinguished. In order to assess the magnitude of the second phase of cooling, an estimation of the wall temperature is made, ignoring the effect of second phase of cooling, and this temperature is compared with the actual temperature. This comparison gives a glimpse of the magnitude of the second phase of cooling that we refer to as additional effects. Estimation of the wall temperature can be obtained assuming that $\dot{q}_a$ is a function of wall temperature alone and not that of blowing rate $\dot{m}_W$.[8] After going through some algebra one can arrive at

$$T_W^{est} = \frac{\dot{m}_W T_C + C_{h0} T_r}{\dot{m}_W + C_{h0}} \tag{3}$$

where C_{h0} is the Stanton number when there is no gas injection.

In Figs. 3a–3d, the ratio T_W/T_W^{est} is plotted along the flat plate for different blowing rates and freestream conditions. For smaller blowing rates, the actual wall temperature is more or less equal to the estimated wall temperature, and hence, the magnitude of the additional effects is small. As the blowing rate is increased, the additional effects become progressively important, particularly towards the end of the flat plate. At large blowing rates, two facts are noticed. In the region towards the end of the plate, the wall temperature is much less than the estimated temperature. In regions close to the leading edge, two opposite effects become important. One is the additional effect described earlier, due to which the wall temperature has to come down below the estimated temperature. At the same time, due to blowing, the boundary layer becomes thick and as a consequence the viscous interaction increases. As a result of increased heat load due to viscous interaction, the wall temperature also increases. Since the two effects are opposite in nature, the wall temperature will remain close to the estimated temperature. The effect of Mach number is not significant at lower blowing rates as observed in Fig. 3a. But the additional effects become important even at the lower blowing rates as the freestream Reynolds number increases, because the thickening of the boundary layer becomes more significant at higher Reynolds numbers. At higher blowing rates and towards the end of the plate the additional effects become stronger at higher Mach numbers. But closer to the leading edge the ratio increases as M_∞ increases. This could be due to stronger viscous interaction at higher M_∞. As the freestream Reynolds number increases, the region where the viscous interaction is important becomes smaller and the ratio decreases with x. For $Re_\infty = 5 \times 10^6$ and 10^7, this ratio decreases sharply with x and then increases slightly with x. The increase in this ratio is because the actual wall temperature remains constant with x (minimum value attainable for that coolant temperature), but the estimated wall temperature keeps decreasing with x (due to a decrease in C_{h0} with x).

Conclusions

Analysis of transpiration cooling over a flat plate at hypersonic Mach numbers is made using full Navier–Stokes equations. A new criterion was developed for determining a relevant range of blowing rates and it was very useful in the parametric analysis. The wall temperature decreases with increase in blowing rate, but this effect is not uniform along the plate. Larger effect was found away from the leading edge. The relative change in wall temperature E_T was more strongly affected by blowing at higher freestream Reynolds number. The estimated temperature analysis was useful in determining the magnitude of the second phase of cooling. It was observed that the additional effects are significant away from the leading edge. Also, these effects become more significant at higher Reynolds numbers.

References

[1]McConarty, W. A., and Anthony, F. M., "Design and Evaluation of Active Cooling Systems for Mach 6 Cruise Vehicles Wings," NASA CR-1916, 1971.

[2]Yoshikawa, K. K., "Linearised Theory of Stagnation Point Heat and Mass Transfer at Hypersonic Speeds," NASA TN-D 5246, 1969.

[3]Sreekanth, and Reddy, N. M., "Transpiration Cooling Analysis at Hypersonic Mach Numbers Using Navier-Stokes Equations," AIAA Paper 94-2075, June 1994.

[4]Sreekanth, "Transpiration Cooling Analysis at Hypersonic Mach Numbers Using Navier-Stokes Equations," Ph.D. Dissertation, Indian Inst. of Science, Bangalore, India, Dec. 1993.

[5]Roe, P. L., "Approximate Riemann Solvers, Parameter Vectors and Difference Schemes," *Journal of Computational Physics*, Vol. 43, 1981, pp. 357–372.

[6]Anderson, W. K., Thomas, J. L., and Van Leer, B., "A Comparison of Finite Volume Flux Vector Splittings for the Euler Equations," AIAA Paper 85-0122, Jan. 1985.
[7]Peyret, R., and Taylor, T. D., "Computational Methods for Fluid Flow," Springer-Verlag, New York, 1983, pp. 108-112.
[8]Blottner, F. G., "Accurate Navier-Stokes Results for the Hypersonic Flow over a Spherical Nose Tip," *Journal of Space Crafts*, Vol. 27, No. 2, 1990, pp. 113-122.

Thermal Stratification Effects Near a Vertical Ice Slab in Cold Water

David J. Kukulka*
State University of New York at Buffalo, Buffalo, New York 14222
John Lamb†
Consolidated Edison, Buchanan, New York 10511
and
Joseph C. Mollendorf‡
State University of New York at Buffalo, Buffalo, New York 14260

Introduction

NATURAL convection flows near ice surfaces melting in pure water have been previously studied by various investigators. Codegone[1] was apparently the first to demonstrate convective reversals or inversions around the density extremum. Ede[2] performed the first detailed heat transfer measurements of density inversions.

Wilson and Vyas[3] melted ice in pure water and measured flow velocities using an optical technique that employed a thymol blue pH solution. Their results suggest upward flows for water temperatures below 4.7°C and entirely downward flows for temperatures above 7.0°C. For intermediate temperatures, an oscillatory dual flow regime was indicated. In addition, they found that as the temperature increased from 4.7°C, the oscillatory dual flow phenomenon was increasingly prevalent, with a maximum downward velocity being reached at 5.6°C. Wilson and Lee[4] presented a steady-state, two-dimensional finite difference analysis for the heat and momentum transfer of a semi-infinite vertical ice sheet at 0°C, melting into fresh water. Density varied with local temperature, while the other fluid properties were assumed to be constant and evaluated at the ambient temperature. The results showed three distinctive steady flow regimes characterized by ambient temperatures t_a: upward flow for $t_a \leq 4.5$°C, downward flow for $t_a \geq 6.0$°C, and dual or bidirectional flow for $5.7 \leq t_a \leq 6.0$°C. In the range 4.5°C $< t_a < 5.7$°C, the solution failed to converge. Wilson and Lee[4] suggest that this could be a failure of the steady-state theory being applied to model a phenomena that is inherently unsteady.

El-henawy et al.[5] theoretically studied the laminar boundary-layer flow adjacent to a heated or cooled, vertical flat surface, submerged in unstratified quiescent cold water. Their results demonstrate the existence of multiple steady-state solutions in a natural convection flow. Multiple steady states were discovered in two regions: $0.15149 \leq R \leq 0.15180$ (largely upflow with outside flow reversals) and $0.29181 \leq R \leq 0.45402$ (largely downflow with inside flow reversals). The density extremum parameter R is defined as $(t_m - t_a)/(t_0 - t_a)$, with t_m being the temperature at maximum density and t_0 the ice-liquid interface temperature. It is possible there is a relationship between the multiple steady-state solutions and the observed unsteadiness in this work. For Prandtl number Pr equal to 11.6, El-henawy et al.[5] narrowed the width of the gap where calculations were not possible to $0.1518 < R < 0.29181$. El-henawy et al.[6] developed a new approach to determine the stability of multiple steady-state similarity solutions and applied it to vertical plane surfaces in cold water. Wang and Wang[7] studied a laminar buoyancy-induced plane flow near a vertical ice wall melting in cold pure water. Their computed results show that no solution can be found in the range $0.153298 < R < 0.294322$. Rationale for the existence of this gap is discussed and comparisons are made to previous investigators.[4,5] Hwang et al.[8] presented the first hydrodynamic stability analysis for a vertical plate in cold water in the range $0.29181 \leq R \leq 0.50$. In this range the inside buoyancy force reversals exert a strong influence upon the flow.

Experiments are performed herein to determine the effect of the gradient of thermal stratification on the anomalous unsteadiness near a vertical ice slab melting in cold water. An evaluation of tank-size effects on the influence of the relative configurational stability of the various predicted multiple steady states is made. That is to say, does tank size and/or the associated ambient thermal stratification cause the unsteadiness previously observed. Experiments are performed in the gap, $0.15180 < R < 0.29181$, where numerical calculations were not previously possible, and in the region, $0.29181 \leq R \leq 0.45402$, where multiple steady-state solutions were demonstrated.

Experimental Procedure

The present experimental investigation consisted of the visualization and the determination of the associated melting rates m of the buoyancy-induced flow caused by the melting

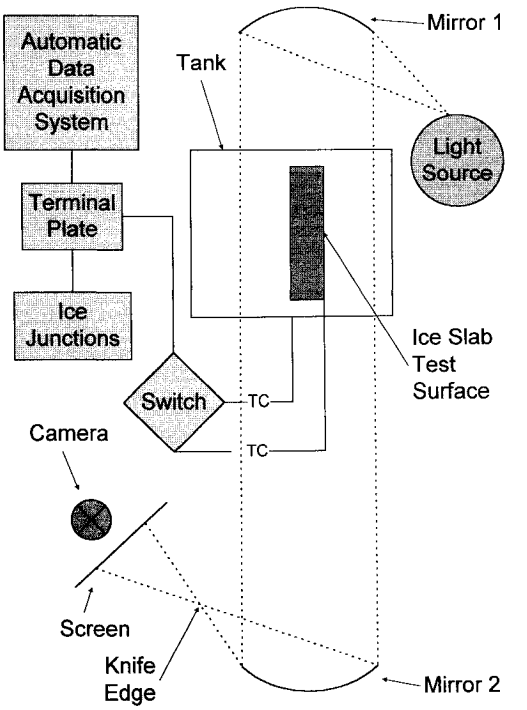

Fig. 1 Experimental layout showing the schlieren optical system.

Received Sept. 20, 1993; revision received Nov. 10, 1994; accepted for publication Nov. 10, 1994.

*Associate Professor, Department of Mechanical Engineering Technology, 1300 Elmwood Ave.
†Project Engineer, Indian Point Station, Broadway & Bleakley Ave.
‡Professor, Department of Mechanical and Aerospace Engineering.